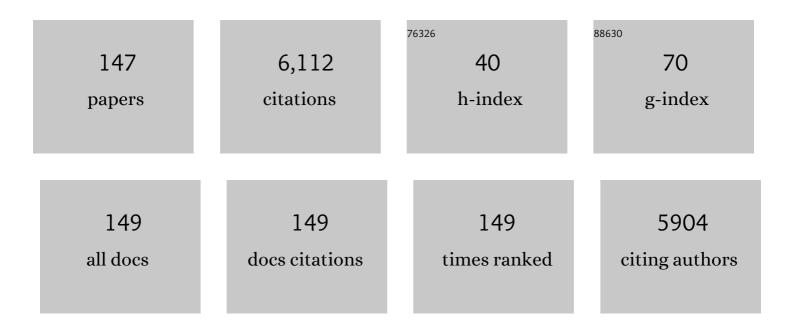
## Nabeel B Nabulsi

List of Publications by Year in descending order

Source: https://exaly.com/author-pdf/1499126/publications.pdf Version: 2024-02-01



NAREEL R NARIUSI

#	Article	IF	CITATIONS
1	Imaging synaptic density in the living human brain. Science Translational Medicine, 2016, 8, 348ra96.	12.4	343
2	Deficits in Prefrontal Cortical and Extrastriatal Dopamine Release in Schizophrenia. JAMA Psychiatry, 2015, 72, 316.	11.0	304
3	Assessing Synaptic Density in Alzheimer Disease With Synaptic Vesicle Glycoprotein 2A Positron Emission Tomographic Imaging. JAMA Neurology, 2018, 75, 1215.	9.0	304
4	Lower synaptic density is associated with depression severity and network alterations. Nature Communications, 2019, 10, 1529.	12.8	277
5	Imaging robust microglial activation after lipopolysaccharide administration in humans with PET. Proceedings of the National Academy of Sciences of the United States of America, 2015, 112, 12468-12473.	7.1	265
6	Synthesis and Preclinical Evaluation of <sup>11</sup> C-UCB-J as a PET Tracer for Imaging the Synaptic Vesicle Glycoprotein 2A in the Brain. Journal of Nuclear Medicine, 2016, 57, 777-784.	5.0	197
7	The neuroinflammation marker translocator protein is not elevated in individuals with mild-to-moderate depression: A [11C]PBR28 PET study. Brain, Behavior, and Immunity, 2013, 33, 131-138.	4.1	180
8	In vivo measurement of widespread synaptic loss in Alzheimer's disease with SV2A PET. Alzheimer's and Dementia, 2020, 16, 974-982.	0.8	170
9	Sex Differences in the Brain's Dopamine Signature of Cigarette Smoking. Journal of Neuroscience, 2014, 34, 16851-16855.	3.6	145
10	Kinetic evaluation and test–retest reproducibility of [ <sup>11</sup> C]UCB-J, a novel radioligand for positron emission tomography imaging of synaptic vesicle glycoprotein 2A in humans. Journal of Cerebral Blood Flow and Metabolism, 2018, 38, 2041-2052.	4.3	143
11	Brivaracetam, a selective highâ€affinity synaptic vesicle protein 2A ( <scp>SV</scp> 2A) ligand with preclinical evidence of high brain permeability and fast onset of action. Epilepsia, 2016, 57, 201-209.	5.1	130
12	PET imaging of the effects of age and cocaine on the norepinephrine transporter in the human brain using (S,S)-[ <sup>11</sup> C]O-methylreboxetine and HRRT. Synapse, 2010, 64, 30-38.	1.2	112
13	Synaptic Changes in Parkinson Disease Assessed with in vivo Imaging. Annals of Neurology, 2020, 87, 329-338.	5.3	112
14	Altered metabotropic glutamate receptor 5 markers in PTSD: In vivo and postmortem evidence. Proceedings of the National Academy of Sciences of the United States of America, 2017, 114, 8390-8395.	7.1	107
15	Preferential binding to dopamine D3 over D2 receptors by cariprazine in patients with schizophrenia using PET with the D3/D2 receptor ligand [11C]-(+)-PHNO. Psychopharmacology, 2016, 233, 3503-3512.	3.1	101
16	PET imaging of synaptic density: A new tool for investigation of neuropsychiatric diseases. Neuroscience Letters, 2019, 691, 44-50.	2.1	85
17	Kinetic Modeling of the Serotonin 5-HT <sub>1B</sub> Receptor Radioligand [ <sup>11</sup> C]P943 in Humans. Journal of Cerebral Blood Flow and Metabolism, 2010, 30, 196-210.	4.3	83
18	In Vivo Ketamine-Induced Changes in [ 11 C]ABP688 Binding to Metabotropic Glutamate Receptor Subtype 5. Biological Psychiatry, 2015, 77, 266-275.	1.3	82

#	Article	IF	CITATIONS
19	Synthesis and Evaluation of 11C-LY2795050 as a κ-Opioid Receptor Antagonist Radiotracer for PET Imaging. Journal of Nuclear Medicine, 2013, 54, 455-463.	5.0	80
20	Assessment of a white matter reference region for <sup>11</sup> C-UCB-J PET quantification. Journal of Cerebral Blood Flow and Metabolism, 2020, 40, 1890-1901.	4.3	77
21	Affinity and selectivity of [ <sup>11</sup> C]â€(+)â€PHNO for the D3 and D2 receptors in the rhesus monkey brain in vivo. Synapse, 2012, 66, 489-500.	1.2	74
22	Effects of age, BMI and sex on the glial cell marker TSPO — a multicentre [11C]PBR28 HRRT PET study. European Journal of Nuclear Medicine and Molecular Imaging, 2019, 46, 2329-2338.	6.4	70
23	Synthesis and <i>in Vivo</i> Evaluation of a Novel PET Radiotracer for Imaging of Synaptic Vesicle Glycoprotein 2A (SV2A) in Nonhuman Primates. ACS Chemical Neuroscience, 2019, 10, 1544-1554.	3.5	70
24	Imaging Glutamate Homeostasis in Cocaine Addiction with the Metabotropic Glutamate Receptor 5 Positron Emission Tomography Radiotracer [11C]ABP688 and Magnetic Resonance Spectroscopy. Biological Psychiatry, 2014, 75, 165-171.	1.3	66
25	First-in-Human Evaluation of <sup>18</sup> F-SynVesT-1, a Radioligand for PET Imaging of Synaptic Vesicle Glycoprotein 2A. Journal of Nuclear Medicine, 2021, 62, 561-567.	5.0	60
26	PTSD is associated with neuroimmune suppression: evidence from PET imaging and postmortem transcriptomic studies. Nature Communications, 2020, 11, 2360.	12.8	56
27	Synaptic density and cognitive performance in Alzheimer's disease: A PET imaging study with [ <sup>11</sup> C]UCBâ€J. Alzheimer's and Dementia, 2022, 18, 2527-2536.	0.8	55
28	Evaluation of the agonist PET radioligand [11C]GR103545 to image kappa opioid receptor in humans: Kinetic model selection, test–retest reproducibility and receptor occupancy by the antagonist PF-04455242. NeuroImage, 2014, 99, 69-79.	4.2	54
29	Association of Aβ deposition and regional synaptic density in early Alzheimer's disease: a PET imaging study with [11C]UCB-J. Alzheimer's Research and Therapy, 2021, 13, 11.	6.2	53
30	Reduced synaptic vesicle protein 2A binding in temporal lobe epilepsy: A [ <sup>11</sup> C]UCBâ€J positron emission tomography study. Epilepsia, 2020, 61, 2183-2193.	5.1	51
31	In vivo evidence of lower synaptic vesicle density in schizophrenia. Molecular Psychiatry, 2021, 26, 7690-7698.	7.9	51
32	Evaluation of [11C]MRB for assessment of occupancy of norepinephrine transporters: Studies with atomoxetine in non-human primates. NeuroImage, 2011, 56, 268-279.	4.2	50
33	Phosphodiesterase 10A PET Radioligand Development Program: From Pig to Human. Journal of Nuclear Medicine, 2014, 55, 595-601.	5.0	50
34	lnÂvivo variation in same-day estimates of metabotropic glutamate receptor subtype 5 binding using [ <sup>11</sup> C]ABP688 and [ <sup>18</sup> F]FPEB. Journal of Cerebral Blood Flow and Metabolism, 2017, 37, 2716-2727.	4.3	49
35	Receptor Occupancy of the Â-Opioid Antagonist LY2456302 Measured with Positron Emission Tomography and the Novel Radiotracer 11C-LY2795050. Journal of Pharmacology and Experimental Therapeutics, 2016, 356, 260-266.	2.5	47
36	Metabotropic Glutamate Receptor 5 and Glutamate Involvement in Major Depressive Disorder: A Multimodal Imaging Study. Biological Psychiatry: Cognitive Neuroscience and Neuroimaging, 2017, 2, 449-456.	1.5	47

#	Article	lF	CITATIONS
37	A singleâ€center, openâ€label positron emission tomography study to evaluate brivaracetam and levetiracetam synaptic vesicle glycoprotein 2A binding in healthy volunteers. Epilepsia, 2019, 60, 958-967.	5.1	45
38	Evaluation of <sup>11</sup> C-BU99008, a PET Ligand for the Imidazoline <sub>2</sub> Binding Sites in Rhesus Brain. Journal of Nuclear Medicine, 2014, 55, 838-844.	5.0	44
39	Age-related changes in binding of the D2/3 receptor radioligand [11C](+)PHNO in healthy volunteers. Neurolmage, 2016, 130, 241-247.	4.2	43
40	Dose-Related Target Occupancy and Effects on Circuitry, Behavior, and Neuroplasticity of the Glycine Transporter-1 Inhibitor PF-03463275 in Healthy and Schizophrenia Subjects. Biological Psychiatry, 2018, 84, 413-421.	1.3	43
41	Comparison of [ <sup>11</sup> C]UCB-J and [ <sup>18</sup> F]FDC PET in Alzheimer's disease: A tracer kinetic modeling study. Journal of Cerebral Blood Flow and Metabolism, 2021, 41, 2395-2409.	4.3	43
42	Studies of the metabotropic glutamate receptor 5 radioligand [ <sup>11</sup> C]ABP688 with <i>N</i> -acetylcysteine challenge in rhesus monkeys. Synapse, 2013, 67, 489-501.	1.2	42
43	Kinetic Modeling of 11C-LY2795050, A Novel Antagonist Radiotracer for PET Imaging of the Kappa Opioid Receptor in Humans. Journal of Cerebral Blood Flow and Metabolism, 2014, 34, 1818-1825.	4.3	42
44	Decreased norepinephrine transporter availability in obesity: Positron Emission Tomography imaging with (S,S)-[11C]O-methylreboxetine. NeuroImage, 2014, 86, 306-310.	4.2	41
45	High-resolution imaging of brain 5-HT1B receptors in the rhesus monkey using [11C]P943. Nuclear Medicine and Biology, 2010, 37, 205-214.	0.6	40
46	Microglial depletion and activation: A [11C]PBR28 PET study in nonhuman primates. EJNMMI Research, 2017, 7, 59.	2.5	39
47	OCD is associated with an altered association between sensorimotor gating and cortical and subcortical 5-HT1b receptor binding. Journal of Affective Disorders, 2016, 196, 87-96.	4.1	38
48	Synthesis and in vivo evaluation of [18F]UCB-J for PET imaging of synaptic vesicle glycoprotein 2A (SV2A). European Journal of Nuclear Medicine and Molecular Imaging, 2019, 46, 1952-1965.	6.4	38
49	PET imaging reveals lower kappa opioid receptor availability in alcoholics but no effect of age. Neuropsychopharmacology, 2018, 43, 2539-2547.	5.4	37
50	Kappa-opioid receptors, dynorphin, and cocaine addiction: a positron emission tomography study. Neuropsychopharmacology, 2019, 44, 1720-1727.	5.4	36
51	Test–Retest Reproducibility of Binding Parameters in Humans with <sup>11</sup> C-LY2795050, an Antagonist PET Radiotracer for the l̂º Opioid Receptor. Journal of Nuclear Medicine, 2015, 56, 243-248.	5.0	35
52	Use of Electronic Cigarettes Leads to Significant Beta2-Nicotinic Acetylcholine Receptor Occupancy: Evidence From a PET Imaging Study. Nicotine and Tobacco Research, 2018, 20, 425-433.	2.6	35
53	First-in-Human Assessment of <sup>11</sup> C-LSN3172176, an M1 Muscarinic Acetylcholine Receptor PET Radiotracer. Journal of Nuclear Medicine, 2021, 62, 553-560.	5.0	35
54	Determination of the In Vivo Selectivity of a New κ-Opioid Receptor Antagonist PET Tracer <sup>11</sup> C-LY2795050 in the Rhesus Monkey. Journal of Nuclear Medicine, 2013, 54, 1668-1674.	5.0	34

#	Article	IF	CITATIONS
55	Quantification of myocardial blood flow with 82Rb: Validation with 15O-water using time-of-flight and point-spread-function modeling. EJNMMI Research, 2016, 6, 68.	2.5	34
56	Age-Related Change in 5-HT <sub>6</sub> Receptor Availability in Healthy Male Volunteers Measured with <sup>11</sup> C-GSK215083 PET. Journal of Nuclear Medicine, 2018, 59, 1445-1450.	5.0	34
57	In vivo evidence for dysregulation of mGluR5 as a biomarker of suicidal ideation. Proceedings of the National Academy of Sciences of the United States of America, 2019, 116, 11490-11495.	7.1	34
58	Synthesis and Preclinical Evaluation of an <sup>18</sup> F-Labeled Synaptic Vesicle Glycoprotein 2A PET Imaging Probe: [ <sup>18</sup> F]SynVesT-2. ACS Chemical Neuroscience, 2020, 11, 592-603.	3.5	34
59	PET imaging reveals sex differences in kappa opioid receptor availability in humans, in vivo. American Journal of Nuclear Medicine and Molecular Imaging, 2016, 6, 205-14.	1.0	34
60	Regional and source-based patterns of [ 11 C]-(+)-PHNO binding potential reveal concurrent alterations in dopamine D 2 and D 3 receptor availability in cocaine-use disorder. NeuroImage, 2017, 148, 343-351.	4.2	32
61	Preliminary in vivo evidence of lower hippocampal synaptic density in cannabis use disorder. Molecular Psychiatry, 2021, 26, 3192-3200.	7.9	32
62	Determination of In Vivo <i>B</i> <sub>max</sub> and <i>K</i> <sub>d</sub> for <sup>11</sup> C-GR103545, an Agonist PET Tracer for κ-Opioid Receptors: A Study in Nonhuman Primates. Journal of Nuclear Medicine, 2013, 54, 600-608.	5.0	31
63	Determination of receptor occupancy in the presence of mass dose: [11C]GSK189254 PET imaging of histamine H3 receptor occupancy by PF-03654746. Journal of Cerebral Blood Flow and Metabolism, 2017, 37, 1095-1107.	4.3	31
64	PET imaging of mGluR5 in Alzheimer's disease. Alzheimer's Research and Therapy, 2020, 12, 15.	6.2	29
65	Cortical β-amyloid burden, gray matter, and memory in adults at varying APOE ε4 risk for Alzheimer's disease. Neurobiology of Aging, 2018, 61, 207-214.	3.1	28
66	Binding of the synaptic vesicle radiotracer [ <sup>11</sup> C]UCB-J is unchanged during functional brain activation using a visual stimulation task. Journal of Cerebral Blood Flow and Metabolism, 2021, 41, 1067-1079.	4.3	28
67	[11C]Glycylsarcosine: synthesis and in vivo evaluation as a PET tracer of PepT2 transporter function in kidney of PepT2 null and wild-type mice. Bioorganic and Medicinal Chemistry, 2005, 13, 2993-3001.	3.0	27
68	First-in-Human Assessment of the Novel PDE2A PET Radiotracer <sup>18</sup> F-PF-05270430. Journal of Nuclear Medicine, 2016, 57, 1388-1395.	5.0	27
69	The Kappa Opioid Receptor Is Associated With Naltrexone-Induced Reduction of Drinking and Craving. Biological Psychiatry, 2019, 86, 864-871.	1.3	27
70	Sex differences in amphetamine-induced dopamine release in the dorsolateral prefrontal cortex of tobacco smokers. Neuropsychopharmacology, 2019, 44, 2205-2211.	5.4	27
71	[11C]GR103545: novel one-pot radiosynthesis with high specific activity. Nuclear Medicine and Biology, 2011, 38, 215-221.	0.6	26
72	Age Effects on Serotonin Receptor 1B as Assessed by PET. Journal of Nuclear Medicine, 2012, 53, 1411-1414.	5.0	26

#	Article	IF	CITATIONS
73	Kappa opioid receptor binding in major depression: A pilot study. Synapse, 2018, 72, e22042.	1.2	26
74	Imaging human brown adipose tissue under room temperature conditions with 11C-MRB, a selective norepinephrine transporter PET ligand. Metabolism: Clinical and Experimental, 2015, 64, 747-755.	3.4	25
75	A preliminary study of dopamine D2/3 receptor availability and social status in healthy and cocaine dependent humans imaged with [11C](+)PHNO. Drug and Alcohol Dependence, 2015, 154, 167-173.	3.2	25
76	Association of entorhinal cortical tau deposition and hippocampal synaptic density in older individuals with normal cognition and early Alzheimer's disease. Neurobiology of Aging, 2022, 111, 44-53.	3.1	25
77	Imaging the effect of ketamine on synaptic density (SV2A) in the living brain. Molecular Psychiatry, 2022, 27, 2273-2281.	7.9	25
78	Dopamine D3 receptor antagonists: The quest for a potentially selective PET ligand. Part 3: Radiosynthesis and in vivo studies. Bioorganic and Medicinal Chemistry Letters, 2009, 19, 5056-5059.	2.2	24
79	Assessment of test-retest reproducibility of [18F]SynVesT-1, a novel radiotracer for PET imaging of synaptic vesicle glycoprotein 2A. European Journal of Nuclear Medicine and Molecular Imaging, 2021, 48, 1327-1338.	6.4	23
80	Evaluation of PET Brain Radioligands for Imaging Pancreatic β-Cell Mass: Potential Utility of 11C-(+)-PHNO. Journal of Nuclear Medicine, 2018, 59, 1249-1254.	5.0	22
81	Social status and demographic effects of the kappa opioid receptor: a PET imaging study with a novel agonist radiotracer in healthy volunteers. Neuropsychopharmacology, 2019, 44, 1714-1719.	5.4	22
82	Assessing the sensitivity of [ <sup>11</sup> C]p943, a novel 5â€HT <sub>IB</sub> radioligand, to endogenous serotonin release. Synapse, 2011, 65, 1113-1117.	1.2	21
83	PET Imaging of Pancreatic Dopamine D <sub>2</sub> and D <sub>3</sub> Receptor Density with <sup>11</sup> C-(+)-PHNO in Type 1 Diabetes. Journal of Nuclear Medicine, 2020, 61, 570-576.	5.0	19
84	Simplified Quantification of <sup>11</sup> C-UCB-J PET Evaluated in a Large Human Cohort. Journal of Nuclear Medicine, 2021, 62, 418-421.	5.0	19
85	Tracer Kinetic Modeling of [ <sup>11</sup> C]AFM, a New PET Imaging Agent for the Serotonin Transporter. Journal of Cerebral Blood Flow and Metabolism, 2013, 33, 1886-1896.	4.3	17
86	Evaluation of <sup>11</sup> C-LSN3172176 as a Novel PET Tracer for Imaging M <sub>1</sub> Muscarinic Acetylcholine Receptors in Nonhuman Primates. Journal of Nuclear Medicine, 2019, 60, 1147-1153.	5.0	17
87	In vivo 5-HT6 and 5-HT2A receptor availability in antipsychotic treated schizophrenia patients vs. unmedicated healthy humans measured with [11C]GSK215083 PET. Psychiatry Research - Neuroimaging, 2020, 295, 111007.	1.8	17
88	Occupancy of the kappa opioid receptor by naltrexone predicts reduction in drinking and craving. Molecular Psychiatry, 2021, 26, 5053-5060.	7.9	17
89	Evaluation of the Lysophosphatidic Acid Receptor Type 1 Radioligand <sup>11</sup> C-BMT-136088 for Lung Imaging in Rhesus Monkeys. Journal of Nuclear Medicine, 2018, 59, 327-333.	5.0	16
90	Quantification of Positron Emission Tomography Data Using Simultaneous Estimation of the Input Function: Validation with Venous Blood and Replication of Clinical Studies. Molecular Imaging and Biology, 2019, 21, 926-934.	2.6	16

#	Article	IF	CITATIONS
91	A metabolically stable PET tracer for imaging synaptic vesicle protein 2A: synthesis and preclinical characterization of [18F]SDM-16. European Journal of Nuclear Medicine and Molecular Imaging, 2022, 49, 1482-1496.	6.4	16
92	Lower prefrontal cortical synaptic vesicle binding in cocaine use disorder: An exploratory <sup>11</sup> Câ€UCB†positron emission tomography study in humans. Addiction Biology, 2022, 27, e13123.	2.6	16
93	Preclinical Evaluation of <sup>18</sup> F-PF-05270430, a Novel PET Radioligand for the Phosphodiesterase 2A Enzyme. Journal of Nuclear Medicine, 2016, 57, 1448-1453.	5.0	13
94	Measuring the effects of ketamine on mGluR5 using [ <sup>18</sup> F]FPEB and PET. Journal of Cerebral Blood Flow and Metabolism, 2020, 40, 2254-2264.	4.3	13
95	The Effect of Treatment with Guanfacine, an Alpha2 Adrenergic Agonist, on Dopaminergic Tone in Tobacco Smokers: An [11C]FLB457 PET Study. Neuropsychopharmacology, 2018, 43, 1052-1058.	5.4	12
96	[ <sup>11</sup> C]Methionine and [ <sup>11</sup> C]PBR28 as PET Imaging Tracers to Differentiate Metastatic Tumor Recurrence or Radiation Necrosis. Molecular Imaging, 2020, 19, 153601212096866.	1.4	12
97	Imaging the Enzyme 11β-Hydroxysteroid Dehydrogenase Type 1 with PET: Evaluation of the Novel Radiotracer <sup>11</sup> C-AS2471907 in Human Brain. Journal of Nuclear Medicine, 2019, 60, 1140-1146.	5.0	11
98	First in-human PET study and kinetic evaluation of [ <sup>18</sup> F]AS2471907 for imaging 11β-hydroxysteroid dehydrogenase type 1. Journal of Cerebral Blood Flow and Metabolism, 2020, 40, 695-704.	4.3	10
99	Kinetic Modeling and Test–Retest Reproducibility of <sup>11</sup> C-EKAP and <sup>11</sup> C-FEKAP, Novel Agonist Radiotracers for PET Imaging of the l̂º-Opioid Receptor in Humans. Journal of Nuclear Medicine, 2020, 61, 1636-1642.	5.0	10
100	Effect of age on brain metabotropic glutamate receptor subtype 5 measured with [18F]FPEB PET. NeuroImage, 2021, 238, 118217.	4.2	10
101	PET Imaging of Synaptic Vesicle Protein 2A. , 2021, , 993-1019.		10
102	Imaging brain cortisol regulation in PTSD with a target for 11β-hydroxysteroid dehydrogenase type 1. Journal of Clinical Investigation, 2021, 131, .	8.2	10
103	Body Mass Index and Age Effects on Brain 11β-Hydroxysteroid Dehydrogenase Type 1: a Positron Emission Tomography Study. Molecular Imaging and Biology, 2020, 22, 1124-1131.	2.6	9
104	Inverse changes in raphe and cortical 5â€HT 1B receptor availability after acute tryptophan depletion in healthy human subjects. Synapse, 2020, 74, e22159.	1.2	9
105	Separating dopamine D2 and D3 receptor sources of [11C]-(+)-PHNO binding potential: Independent component analysis of competitive binding. NeuroImage, 2020, 214, 116762.	4.2	9
106	A multi species evaluation of the radiation dosimetry of [ 11 C]erlotinib, the radiolabeled analog of a clinically utilized tyrosine kinase inhibitor. Nuclear Medicine and Biology, 2017, 47, 56-61.	0.6	8
107	The Search for a Subtype-Selective PET Imaging Agent for the GABA <sub>A</sub> Receptor Complex: Evaluation of the Radiotracer [ <sup>11</sup> C]ADO in Nonhuman Primates. Molecular Imaging, 2017, 16, 153601211773125.	1.4	8
108	Tobacco Smoking in People Is Not Associated with Altered 18-kDa Translocator Protein Levels: A PET Study. Journal of Nuclear Medicine, 2020, 61, 1200-1204.	5.0	8

#	Article	IF	CITATIONS
109	Human adult and adolescent biodistribution and dosimetry of the synaptic vesicle glycoprotein 2A radioligand 11C-UCB-J. EJNMMI Research, 2020, 10, 83.	2.5	8
110	962. In-vivo Evidence of Decreased Synaptic Density in Schizophrenia: A [11C]UCB-J PET Imaging Study. Biological Psychiatry, 2017, 81, S389.	1.3	7
111	Evaluation of (â€}â€{ <sup>18</sup> <scp>F]F</scp> lubatineâ€specific binding: Implications for reference region approaches. Synapse, 2018, 72, e22016.	1.2	7
112	Binge alcohol use is not associated with alterations in striatal dopamine receptor binding or dopamine release. Drug and Alcohol Dependence, 2019, 205, 107627.	3.2	7
113	Longitudinal imaging of metabotropic glutamate 5 receptors during early and extended alcohol abstinence. Neuropsychopharmacology, 2021, 46, 380-385.	5.4	7
114	Imaging Pituitary Vasopressin 1B Receptor in Humans with the PET Radiotracer <sup>11</sup> C-TASP699. Journal of Nuclear Medicine, 2022, 63, 609-614.	5.0	7
115	A modification to improve the reliability of <scp>[<sup>11</sup>C]CN<sup>â^'</sup></scp> production in the <scp>CE</scp> radiochemistry system. Journal of Labelled Compounds and Radiopharmaceuticals, 2017, 60, 592-595.	1.0	5
116	Quantitative projection of human brain penetration of the H <sub>3</sub> antagonist PF-03654746 by integrating rat-derived brain partitioning and PET receptor occupancy. Xenobiotica, 2017, 47, 119-126.	1.1	5
117	PET Imaging Estimates of Regional Acetylcholine Concentration Variation in Living Human Brain. Cerebral Cortex, 2021, 31, 2787-2798.	2.9	5
118	F149. Preliminary Evidence for Altered Synaptic Density and a Possible Role for Accelerated Ageing in Individuals With MDD as Measured With [11C]UCB-J PET. Biological Psychiatry, 2018, 83, S296.	1.3	4
119	Assessment of transient dopamine responses to smoked cannabis. Drug and Alcohol Dependence, 2021, 227, 108920.	3.2	4
120	Imaging the fetal nonhuman primate brain with SV2A positron emission tomography (PET). European Journal of Nuclear Medicine and Molecular Imaging, 2022, 49, 3679-3691.	6.4	4
121	Initial Experience with PET Imaging of Synaptic Density (SV2A) in Alzheimer's Disease: A New Biomarker for Clinical Trials?. American Journal of Geriatric Psychiatry, 2018, 26, S145-S146.	1.2	3
122	Evaluation of quantitative modeling methods in whole-body, dynamic [C]-erlotinib PET. American Journal of Nuclear Medicine and Molecular Imaging, 2021, 11, 143-153.	1.0	3
123	Feasibility of imaging synaptic density in the human spinal cord using [11C]UCB-J PET. EJNMMI Physics, 2022, 9, 32.	2.7	3
124	Association between cerebrospinal fluid biomarkers of neurodegeneration and PET measurements of synaptic density in Alzheimer's disease. Alzheimer's and Dementia, 2020, 16, e044211.	0.8	2
125	Differences in the association between kappa opioid receptors and pain among Black and White adults with alcohol use disorders. Alcoholism: Clinical and Experimental Research, 2022, 46, 1348-1357.	2.4	2
126	Investigating Age Related Associations of Metabotropic Glutamate Receptor 5 Density Using [ 18 F]FPEB and PET. American Journal of Geriatric Psychiatry, 2017, 25, S96-S97.	1.2	1

#	Article	IF	CITATIONS
127	P1â€469: PET IMAGING OF METABOTROPIC GLUTAMATE RECEPTOR 5 BINDING IN ALZHEIMER'S DISEASE. Alzheimer's and Dementia, 2018, 14, P501.	0.8	1
128	In vivo measurement of widespread synaptic loss and associated tau accumulation in early Alzheimer's disease. Alzheimer's and Dementia, 2020, 16, e037791.	0.8	1
129	Validation of a simplified tissueâ€toâ€reference ratio measurement using SUVR for the assessment of synaptic density alterations in Alzheimer's disease using [ 11 C]UCBâ€J PET. Alzheimer's and Dementia, 2020, 16, e045928.	0.8	1
130	Dopamine D2/3 receptor availability in cocaine use disorder individuals with obesity as measured by [11C]PHNO PET. Drug and Alcohol Dependence, 2021, 220, 108514.	3.2	1
131	Synaptic density is associated with cognitive performance in early Alzheimer's disease: a PET imaging study with [11C]UCB-J. American Journal of Geriatric Psychiatry, 2021, 29, S119-S120.	1.2	1
132	Nicotine patch alters patterns of cigarette smoking-induced dopamine release: Patterns relate to biomarkers associated with treatment response. Nicotine and Tobacco Research, 2022, , .	2.6	1
133	P2â€365: PET IMAGING OF SYNAPTIC DENSITY (SYNAPTIC VESICLE GLYCOPROTEIN 2A, SV2A) IN ALZHEIMER'S DISEASE: INITIAL EXPERIENCE. Alzheimer's and Dementia, 2018, 14, P832.	0.8	0
134	2181 Age-related change in 5-HT6 receptor availability in healthy male volunteers measured with 11C-CSK215083 PET. Journal of Clinical and Translational Science, 2018, 2, 3-4.	0.6	0
135	ICâ€04â€03: PET IMAGING OF METABOTROPIC GLUTAMATE RECEPTOR 5 BINDING IN ALZHEIMER'S DISEASE. Alzheimer's and Dementia, 2018, 14, P8.	0.8	0
136	ICâ€₽â€183: PET IMAGING OF SYNAPTIC DENSITY (SYNAPTIC VESICLE GLYCOPROTEIN 2A, SV2A) IN ALZHEIMER'S DISEASE: INITIAL EXPERIENCE. Alzheimer's and Dementia, 2018, 14, P152.	, 0.8	0
137	S13. IN VIVO EVIDENCE OF REDUCED SYNAPTIC VESICLE DENSITY IN SCHIZOPHRENIA USING [11C] UCB-J PET IMAGING. Schizophrenia Bulletin, 2019, 45, S310-S311.	4.3	0
138	P4â€481: ASSOCIATION BETWEEN ENTORHINAL CORTICAL TAU ACCUMULATION AND HIPPOCAMPAL SYNAPTIC DENSITY IN OLDER INDIVIDUALS WITH NORMAL COGNITION AND EARLY ALZHEIMER'S DISEASE: PRELIMINARY EXPERIENCE. Alzheimer's and Dementia, 2019, 15, P1497.	0.8	0
139	ICâ€Pâ€140: ASSOCIATION BETWEEN MGLUR5 AND SYNAPTIC DENSITY: A MULTIâ€TRACER STUDY IN HEALTHY A AND ALZHEIMER'S DISEASE. Alzheimer's and Dementia, 2019, 15, P115.	AGING	0
140	PBR28 Brain PET imaging with lipopolysaccharide challenge for the study of microglia function in Alzheimer's disease. Alzheimer's and Dementia, 2020, 16, e037792.	0.8	0
141	11Câ€PBR28 brain PET imaging with lipopolysaccharide challenge for the study of microglia function in Alzheimer's disease. Alzheimer's and Dementia, 2020, 16, e043584.	0.8	0
142	Association between cerebral amyloid accumulation and synaptic density in Alzheimer's disease: A multitracer PET study. Alzheimer's and Dementia, 2020, 16, e043631.	0.8	0
143	ASSOCIATION BETWEEN CEREBRAL AMYLOID ACCUMULATION AND SYNAPTIC DENSITY IN ALZHEIMER'S DISEASE: A MULTITRACER PET STUDY. American Journal of Geriatric Psychiatry, 2020, 28, S123-S124.	1.2	0
144	Principal component analysis of synaptic density measured with [11C]UCB-J PET in Alzheimer's disease. American Journal of Geriatric Psychiatry, 2021, 29, S47-S48.	1.2	0

#	Article	IF	CITATIONS
145	Imaging the Effect of Ketamine on Synaptic (SV2A) Density. Biological Psychiatry, 2021, 89, S35.	1.3	0
146	Translational PET Imaging of Spinal Cord Injury with the Serotonin Transporter Tracer [11C]AFM. Molecular Imaging and Biology, 2022, , 1.	2.6	0
147	Assessment of gray matter microstructure and synaptic density in Alzheimer's disease: A multimodal imaging study with DWI and SV2A PET. American Journal of Geriatric Psychiatry, 2022, 30, S26.	1.2	0